

# Experimental Energetics of Large and Extra-Large Pore Zeolites: Pure Silica Beta Polymorph C (BEC) and Ge-containing ITQ-33

L. Wu\*, M. Moliner\*\*, J. Hughes\*, A. Corma\*\*, A. Navrotsky\*

\* Peter A. Rock Thermochemistry Laboratory and NEAT ORU, University of California Davis, Davis, CA 95616, USA

\*\* Instituto de Tecnología Química (UPV-CSIC), Av. Naranjos s/n, E-46022 Valencia, Spain

## Abstract

The enthalpies of formation of the large pore pure silica beta polymorph C (BEC) and the extra-large pore germanosilicate ITQ-33 zeolite are investigated by high temperature oxide melt solution calorimetry. The enthalpies of formation from quartz for two BECs synthesized with different structure directing agents, SDA1 and SDA9 differ by 4 kJ/mol. The two OSDAs produce phases with different properties as well as different energetics for the same framework and composition, due to the different amount of structural defects. Interestingly, the enthalpy of formation of defect-free pure silica BEC perfectly fits the predicted value proposed several years ago for this Ge-free BEC polymorph. Moreover, the enthalpy of formation of ITQ-33 ( $\text{Ge}/(\text{Ge}+\text{Si}) = 0.3$ ) supports the energetic trends seen previously, namely that the enthalpy of formation becomes more endothermic as the content of double-four rings (D4R) increases. The previous trend of energetics of porous materials versus molar volume is supported by the present data, with a diminishing destabilization for very open structures.

## Introduction

The synthesis of open large pore silicates is very attractive for catalytic applications [1]. Together with Faujasite, the most used large pore zeolite presenting a three-dimensional pore topology is the Beta zeolite [2]. This molecular sieve presents two straight large pores with openings of  $6.6 \times 6.7 \text{ \AA}$  and one sinusoidal channel with an effective pore of  $5.6 \times 5.6 \text{ \AA}$  [2]. Interestingly, a third polymorph of Beta zeolite, named Polymorph C (BEC), was theoretically proposed presenting a more open structure, since this polymorph shows a three-dimensional straight large channels ( $7.5 \times 6.3 \text{ \AA}$  and  $6.9 \times 6.0 \text{ \AA}$ ) [2]. BEC zeolite contains D4R cages in its structure, and it was first synthesized as pure germanate [3] or silicogermanate [4] using several organic structure directing agents (OSDA).

Very recently, we have been able to prepare the pure silica BEC polymorph using two different synthetic pathways [5]. Indeed, two different pure silica polymorph

C materials, obtained from SDA1 and SDA9 (see Figure 1), have been prepared. The main differences of SDA9 and SDA1 are ion sizes and charge density, SDA9 is twice as big as SDA1 and carries two positive charges. BEC structure can accommodate two SDA1 in a single unit cell accompanied with two F<sup>-</sup> balancing the charge in two adjacent D4R subunits [5a]. However, in the same structure, two F<sup>-</sup> ions in two D4R subunits cannot balance the four positive charges of two SDA9. To compensate, silicon vacancies produce extra negative charge in the framework, which forms unsaturated Si-O bonds [5b]. The introduction of such defects could bring some additional instability to the BEC structure. <sup>29</sup>Si MAS NMR spectra of these two pure silica BEC zeolites clearly reveal the larger presence of structural defects in pure silica BEC-SDA9 than in BEC-SDA1 (see band at -99 ppm in Figure 2). Thus they may be expected to have slightly different thermodynamic properties.

On the other hand, extra-large pore zeolites contain very large channels defined by rings larger than 12 members [6]. The pore size is in the range of 7-20 Å [6], which is between the pore diameter of microporous and mesoporous materials. It was theoretically predicted that zeolites with large void volumes must contain large number of 3- and 4-rings in their structures [7]. The synthesis of several extra-large pore zeolites, all of them presenting very low framework densities, has been recently achieved thanks to the introduction of germanium atoms in the synthesis gel [8]. Ge substituted zeolites contain Ge-O-Ge and/or Ge-O-Si bond angles, which are more adequate than Si-O-Si to stabilize small cages, such as double-4-rings (D4R) or double-3-rings (D3R) [6]. High surface area and large channels of Ge-silicate materials provide access to bulky molecules, which provides novel potential application in catalysis [6a].

The present work reports a thermodynamic study, using high temperature oxide melt solution calorimetry, of three new zeolites: two pure silica polymorph C (BEC) samples and the Ge-zeolite ITQ-33 with Ge/(Ge+Si) ratio of 0.3. Both types of zeolites have large molar volumes, 40 cm<sup>3</sup>/mol for BEC and 34 cm<sup>3</sup>/mol for ITQ-33. The relative stability of the same structure (BEC) made through different synthesis protocols and organic structure directing agents (OSDAs) was studied. The energetics of ITQ-33 was compared with other Ge-zeolites. The enthalpies of these new large pore zeolites support the previous trend of energetics versus molar volume established for a broad range of porous materials.

## **Experimental Methods**

### **Synthesis, calcination and characterization**

All samples in this study are synthesized following the synthesis methods published previously [5, 6a]. To investigate the enthalpies of the framework without OSDAs, proper calcination must be performed without destroying the framework. Thermal behavior of all samples was first explored by differential scanning calorimetry combined with thermogravimetric analysis (DSC-TGA) to determine appropriate calcination temperatures.

ITQ-33 was analyzed by DSC-TGA (Setaram Labsys) from 20 to 800 °C in O<sub>2</sub> atmosphere with heating rate of 10 °C/min without holding at the highest temperature. The two BEC samples were analyzed from 20 to 550 °C. After calcination, samples were immediately moved into a glovebox under nitrogen to avoid contact with moisture in air. The phases before and after calcination were checked using powder X-ray diffraction (Bruker Avance D8) with Cu K $\alpha$  radiation operated at 40 kV and 40 mA.

### Calorimetry

High temperature oxide melt solution calorimetry was performed for all three calcined samples using a Tian Calvet twin calorimeter and methodology described previously [9, 10]. Samples (2 - 5 mg) were weighed and pressed into pellets in a nitrogen atmosphere glovebox, then the pellets were immediately dropped from room temperature into the calorimeter at 700 °C with molten lead borate (2PbO·B<sub>2</sub>O<sub>3</sub>) solvent. In order to stir the solvent and accelerate dissolution, air was bubbled through the Pt crucible at 10 ml/min and flushed over the solvent at 50 ml/min to remove evolved vapor. The calorimeter was calibrated using the heat content of  $\alpha$ -Al<sub>2</sub>O<sub>3</sub> pellets.

## Results

As TG-DSC curves (Figures 3-5), the pyrolysis of the OSDA of the two BECs occurred at 300 to 450 °C, with BEC(SDA9) showing one pyrolysis step more than BEC(SDA1). The pyrolysis of the OSDA of the ITQ-33 was completed at 200 to 700 °C in several steps. The PXRD patterns for BEC materials and ITQ-33 before and after calcination are shown in Figures 6-8, confirming that the crystalline phases remained after the calcination process.

By using the thermodynamic cycle in Table 1 and drop solution calorimetric data in Table 2, the formation enthalpy from germania and silica (quartz structure) ( $\Delta H_{f,ox}$ ) for ITQ-33 is  $22.12 \pm 0.91$  kJ/mol. The enthalpies of formation from quartz of two BECs are  $17.79 \pm 0.72$  kJ/mol and  $21.73 \pm 2.35$  kJ/mol.

The two BECs with different OSDAs provide a good example to study the influence of the OSDA on structure and thermodynamic stability. BEC-SDA9 is about 4 kJ/mol less stable in enthalpy than BEC-SDA1. According to <sup>29</sup>Si MAS NMR study (see Figure 2), BEC-SDA1 has a more ordered structure whereas BEC-SDA9 has more defects and the energetics reflect this difference. Thus using different OSDAs to introduce structural defects could be a new strategy to modify the structure, energetics, and catalytic activity of a given structure.

In a previous paper, the relationship between enthalpies of formation and (Ge+Si) ratios was studied for Beta and BEC zeolites [11]. In that work, it was observed that the enthalpies of formation relative to quartz become increasingly endothermic in both structures when increasing Ge content (see Figure 9). The enthalpy of pure silica BEC, which was not yet synthesized in that moment, was

extrapolated and estimated to be significantly higher than for Beta or other related pure silica large pore zeolites (as ITQ-7). This higher enthalpy of formation (~16.5 kJ/mol) was claimed as the reason why the pure silica BEC was difficult to be synthesized [11]. However, now, we can prepare pure silica BEC zeolites using very specific OSDAs, which can direct the crystallization of this structure despite its higher enthalpy of formation. If the experimental enthalpy of formation achieved for the pure silica BEC material free of connectivity defects (BEC-SDA1) is plotted in Figure 9, it can be observed that the lineal prediction performed several years ago fits with the experimental value obtained here (~17.7±0.7 kJ/mol).

On the other hand, ITQ-33 is a silicogermanate ( $\text{Ge}/(\text{Ge}+\text{Si}) = 0.30$ ) with an 18 x 10 x 10 member ring channel system, which represents one of largest ring systems known with a framework density of 12.3 T/1,000 Å. The enthalpy of formation from quartz and germania of ITQ-33 is compared to those of ITQ-7, 17, 21, 22 in Figure 10. The formation enthalpy of ITQ-33 is located between ITQ-21 and ITQ-17 with similar Ge content. The previous study of silicogermanate indicated that the enthalpies of formation are more endothermic as Ge content increases [12] and ITQ-33 follows the general trends shown in Figure 11. ITQ-33 has 52 % of the tetrahedral sites involved in double four membered rings (D4MR), compared to 66 % (ITQ-21), 52 % (ITQ-33), 50 % (ITQ-17,-7), and 26 % (ITQ-22) [12]. ITQ-33 follows the trend that the large pore silicogermanate structures with more D4R sites in the framework are less stable than the structures with fewer D4R sites. The longer Ge-O bond compared to Si-O raises the possibility to reduce the strain in large rings in the framework. On the other hand, the smaller bond angle of Ge-O-Ge or Ge-O-Si compared to Si-O-Si enables the formation of more complex ring systems. The larger rings are balanced by smaller ring structures, namely the D4R linkages. The observed structures, though less stable than the pure silica zeolites, probably represent a balance of factors leading to the least unfavorable energetics.

In addition, previous work has shown a monotonic relationship between enthalpies of formation and molar volume of a wide family of porous materials [13]. This relationship is roughly linear for the denser materials but shows a decreasing slope at higher porosity. Figure 12 shows that the large pore zeolites in this study fall on the same trend.

## Conclusion

Enthalpies of formation of BEC-SDA1, BEC-SDA9, and ITQ-33, from component oxides in the quartz structure are reported. The different thermodynamic stability of BEC-SDA9 and BEC-SDA1 reveals the potential of the OSDA in the synthesis of porous structures with different defect concentrations. Very interestingly, the experimental enthalpy of formation calculated for the defect-free pure silica BEC polymorph perfectly fits with the predicted value proposed several years ago. In addition, comparison among ITQ-33, ITQ-22,

ITQ-21, ITQ-17 and ITQ-7 suggests that the molar volume is the main factor governing the stability of Ge-containing zeolites. The content of D4R units is also an indicator of stability of silicogermanates. Structures with more D4R sites in the framework are less stable than those with less. The Ge content affects the enthalpies of formation of the same type of framework in a linear fashion.

## Acknowledgement:

This calorimetric work at UC Davis was supported by the U.S. Department of Energy, grantDE-FG02-05ER15667.

## Reference:

- [1] a) M. E. Davis, *Nature* 2002, 417, 813-821; b) A. Corma, *J. Catal.* 2003, 216, 298-312.
- [2] M. M. J. Treacy, J. M. Newsam, *Nature*. 1988, 332, 249.
- [3] T. Conradsson, M. S. Dadachov, X. D. Zou, *Micropor. Mesopor. Mat.* 2000, 41, 183.
- [4] A. Corma, M. T. Navarro, F. Rey, J. Rius, S. Valencia, *Angew. Chem., Int. Ed.* 2001, 40, 2277.
- [5] a) Á. Cantín, A. Corma, M.J. Díaz-Cabañas, J.L. Jordá, M. Moliner, F. Rey, *Angew. Chem. Int. Ed.*, 45 (2006) 8013-8015, b) M. Moliner, P. Serna, A. Cantín, G.. Sastre, M.J. Díaz-Cabañas, A. Corma, *J. Phys. Chem. C*, 112 (2008) 19547-19554.
- [6] (a) A. Corma, M.J. Diaz-Cabanias, J.L. Jorda, C. Martinez, M. Moliner, *Nature*, 443 (2006) 842-845; (b) A. Corma, M. E. Davis, *ChemPhysChem*, 5, (2004) 304-313; (c) J. Jiang, J. Yu, A. Corma, *Angew. Chem., Int. Ed.*, 49, 2010, 3120-3145.
- [7] G. O. Brunner, W. M. Meier, *Nature* 1989, 337, 146-147.
- [8] a) A. Corma, M. J. Díaz-Cabañas, F. Rey, S. Nicolopoulos, K. Boulahya, *Chem. Commun.* 2004, 1356-1357; b) J. Sun, C. Bonneau, A. Cantín, A. Corma, M. J. Diaz-Cabañas, M. Moliner, D. Zhang, M. Li, X. Zou, *Nature* 2009, 458, 1154-1157; c) J. Jiang, J. L. Jorda, M. J. Díaz-Cabañas, J. Yu, A. Corma, *Angew. Chem., Int. Ed.* 2010, 49, 4986-4988; d) J. Jiang, J. L. Jorda, J. Yu, L. A. Baumes, E. Mugnaioli, M. J. Diaz-Cabanias, U. Kolb, A. Corma, *Science* 2011, 333, 1131-1134; e).A. Corma, M.J. Díaz-Cabañas, J. Jiang, M. Afeworki, D.L. Dorset, S.L. Soled, K.G. Strohmaier, *Proc. Natl. Acad. Sci.*, 107 (2010) 13997-14002.
- [9] A. Navrotsky, *Phys Chem Min*, 2 (1977) 89-104.
- [10] A. Navrotsky, *Phys Chem Min*, 24 (1997) 222-241.
- [11] Q. Li, A. Navrotsky, F. Rey, A. Corma, *Microporous Mesoporous Mater.*, 59 (2003) 177-183.
- [12] Q. Li, A. Navrotsky, F. Rey, A. Corma, *Microporous Mesoporous Mater.*, 74 (2004) 87-92.
- [13] J.T. Hughes, A. Navrotsky, *J. Am. Chem. Soc.*, 133 (2011) 9184-9187.
- [14] P.M. Piccione, C. Laberty, S. Yang, M.A. Camblor, A. Navrotsky, M.E. Davis, *J. Phys. Chem. B*, 104 (2000) 10001-10011.

- [15] I. Kiseleva, A. Navrotsky, I.A. Belitsky, B.A. Fursenko, *Am. Mineral.* 81 (1996) 658.
- [16] R.A. Robie, B.S. Hemingway, *Geo. Surv. Bull.* 2131 (1995) 15.

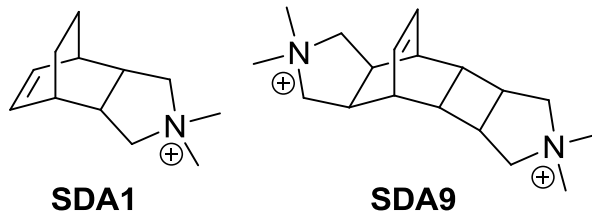


**Figure 1.** Organic structure directing agents SDA1 and SDA9 used in the synthesis of pure silica BEC zeolites

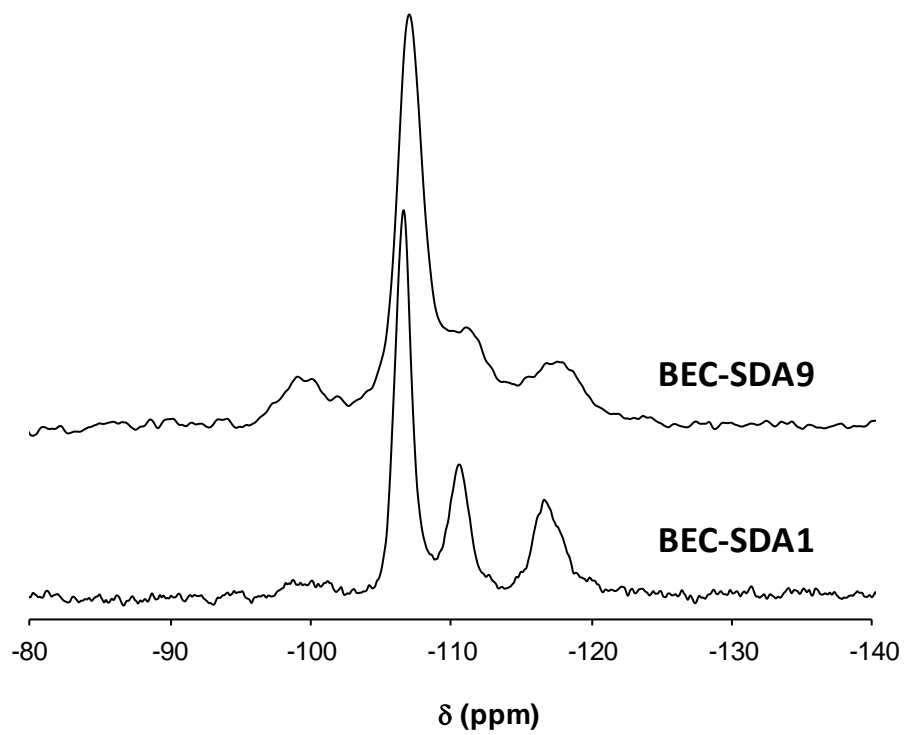


**Figure 2.**  $^{29}\text{Si}$  MAS NMR spectra of pure silica BEC materials



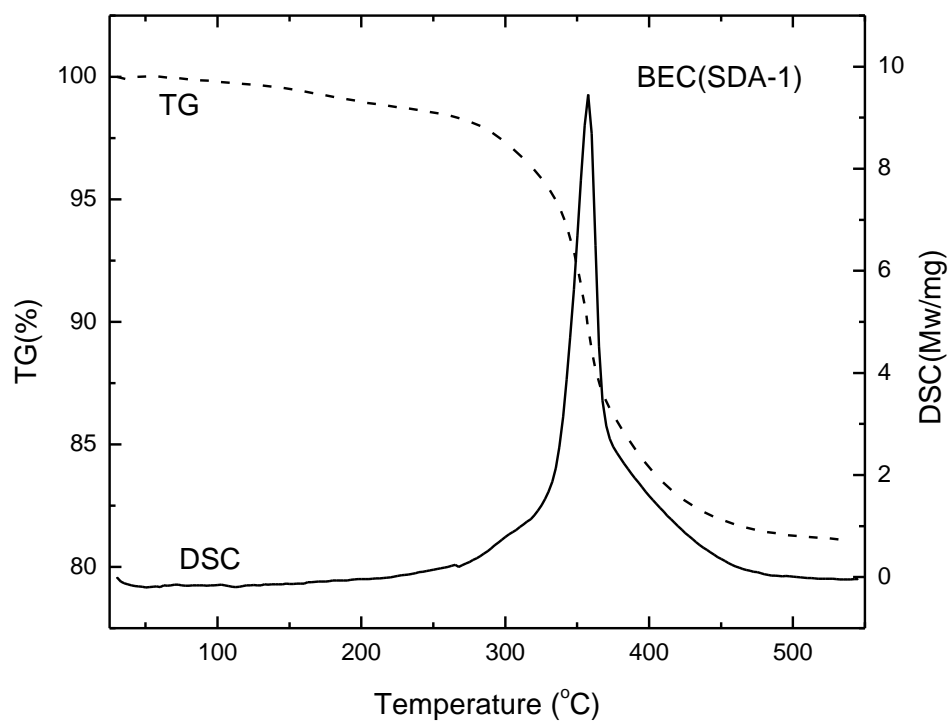


**Figure 3:** DSC-TG curve from 20 to 550 °C for BEC(SDA-1)

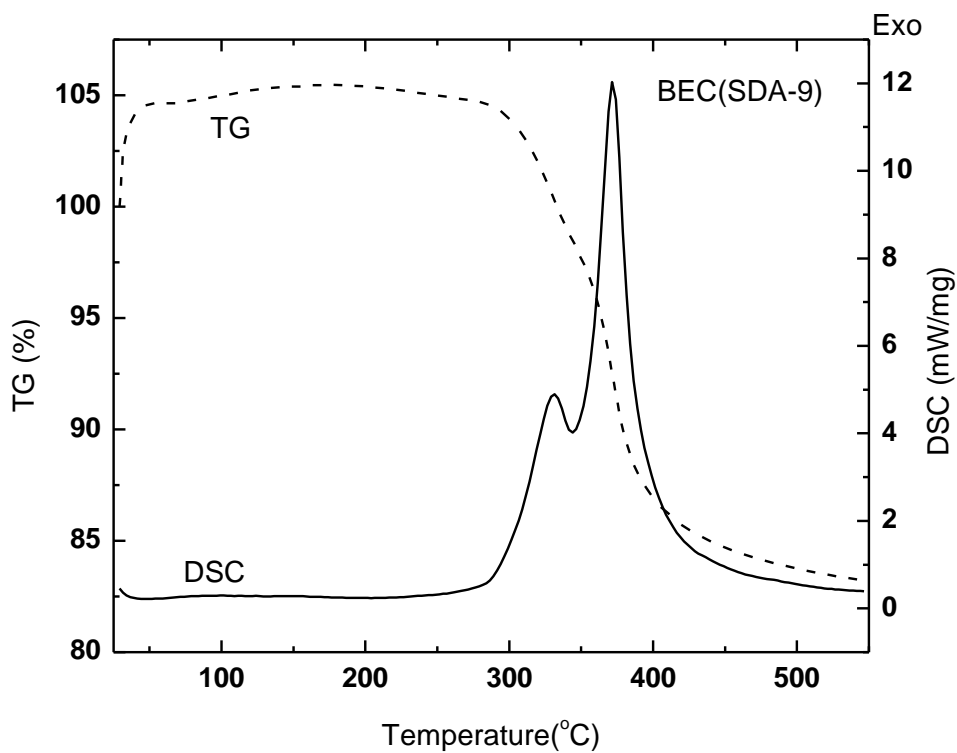


**Figure 4:** DSC-TG curve from 20 to 550 °C for BEC(SDA-9)

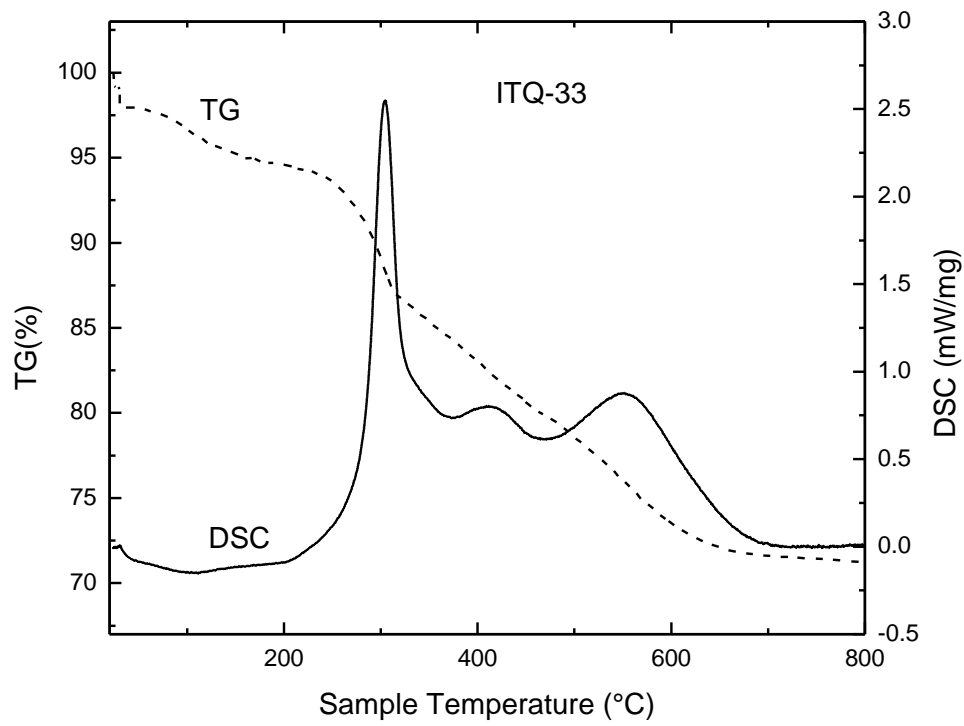


**Figure 5:** DSC-TG curve from 20 to 800°C for ITQ-33

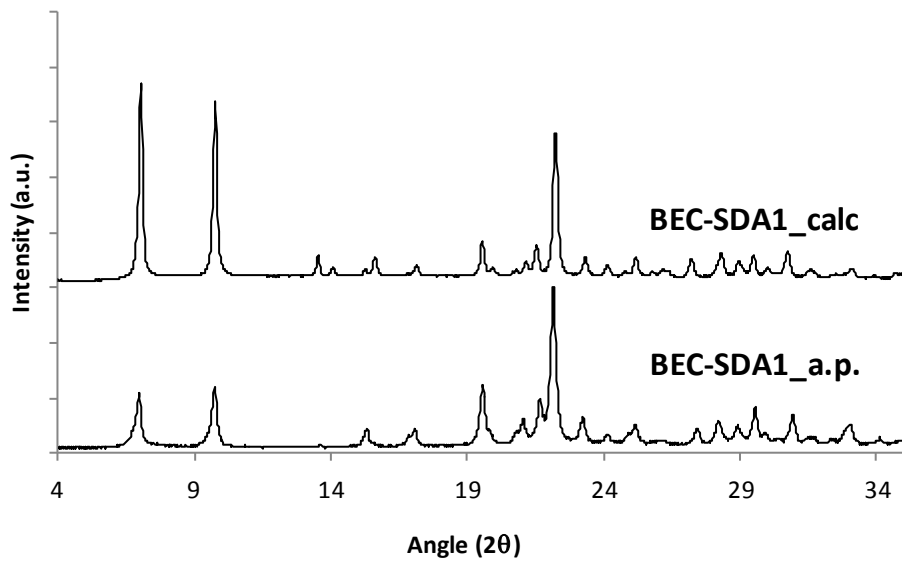


**Figure 6:** PXRD pattern of BEC-SDA1 before and after calcination at 550°C

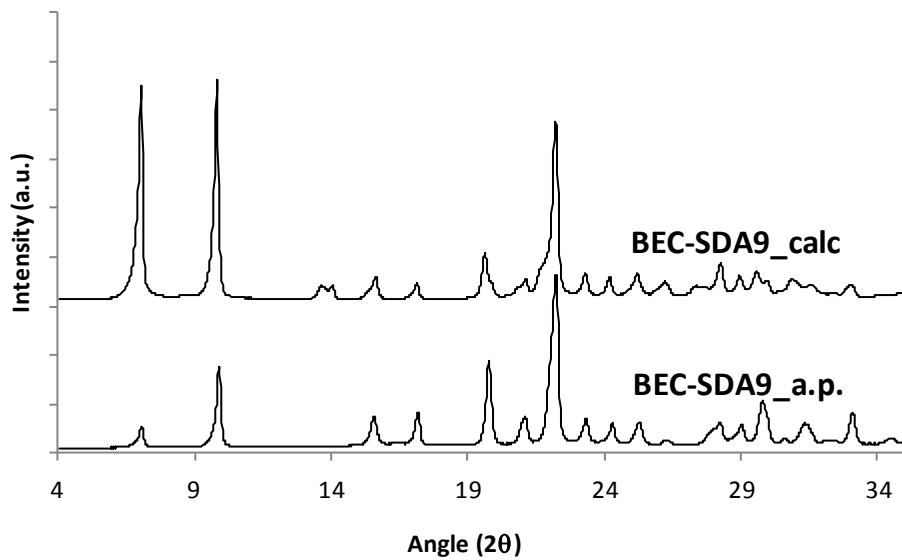


**Figure 7:** PXRD pattern of BEC-SDA9 before and after calcination in oxygen atmosphere

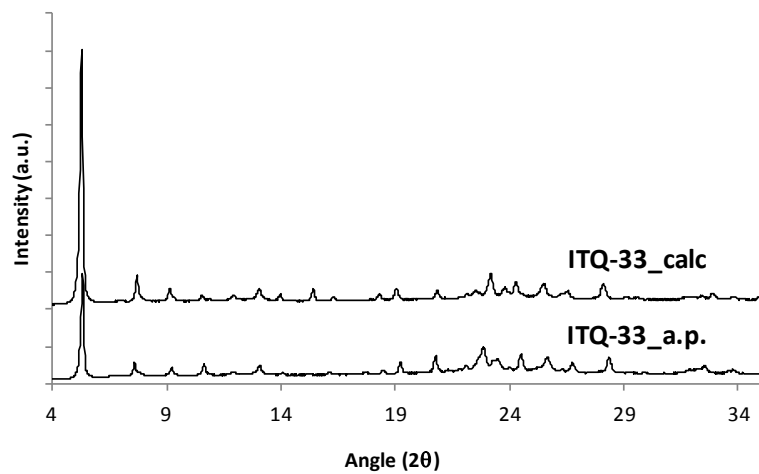


**Figure 8:** PXRD pattern of ITQ-33 before and after calcination at 700°C

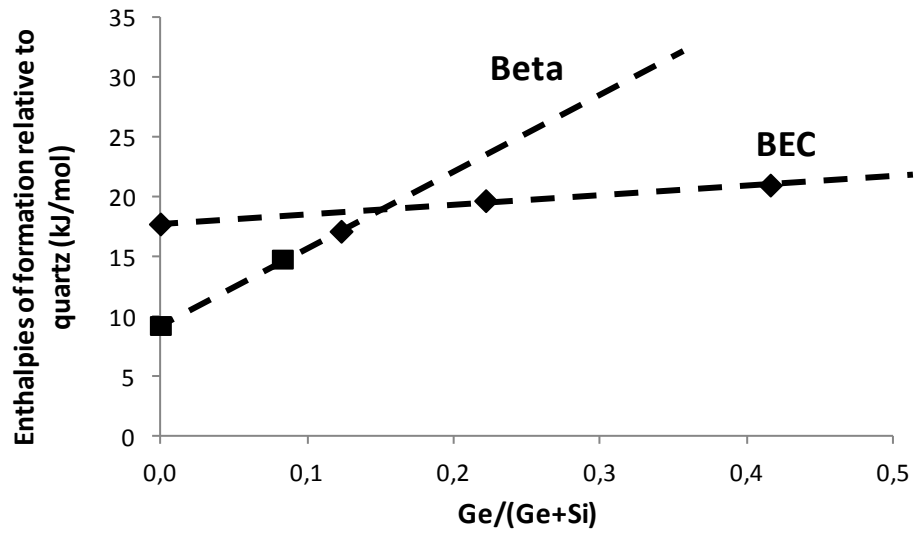


**Figure 9:** Enthalpies of formation relative to a mixture of Germania and silica in the quartz structure as the function of Ge/(Ge+Si) ratio

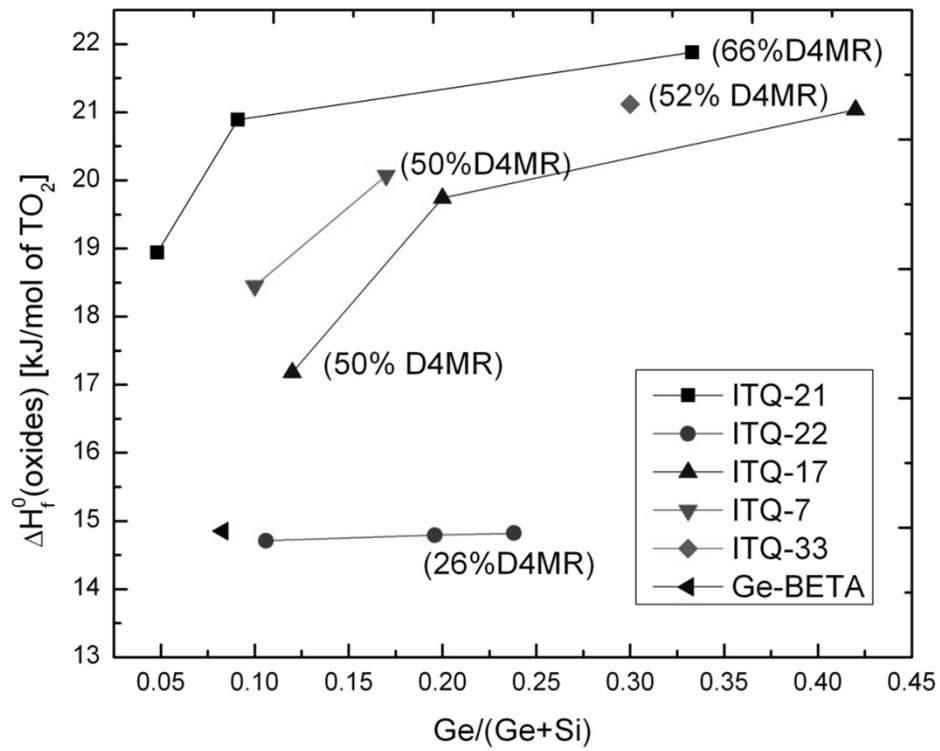


**Figure 10:** Enthalpies of formation from quartz and germania as a function of Ge content for ITQ-21, -22, -17, -7, -33 [14]



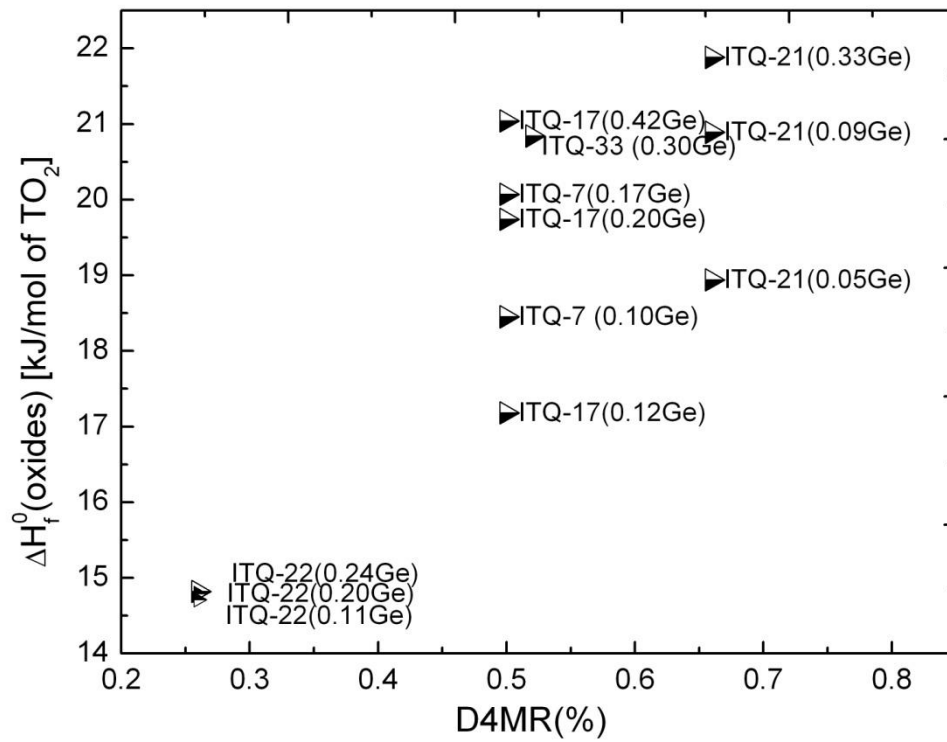


**Figure 11:** Enthalpies of formation of ITQ series versus percent of D4R sites

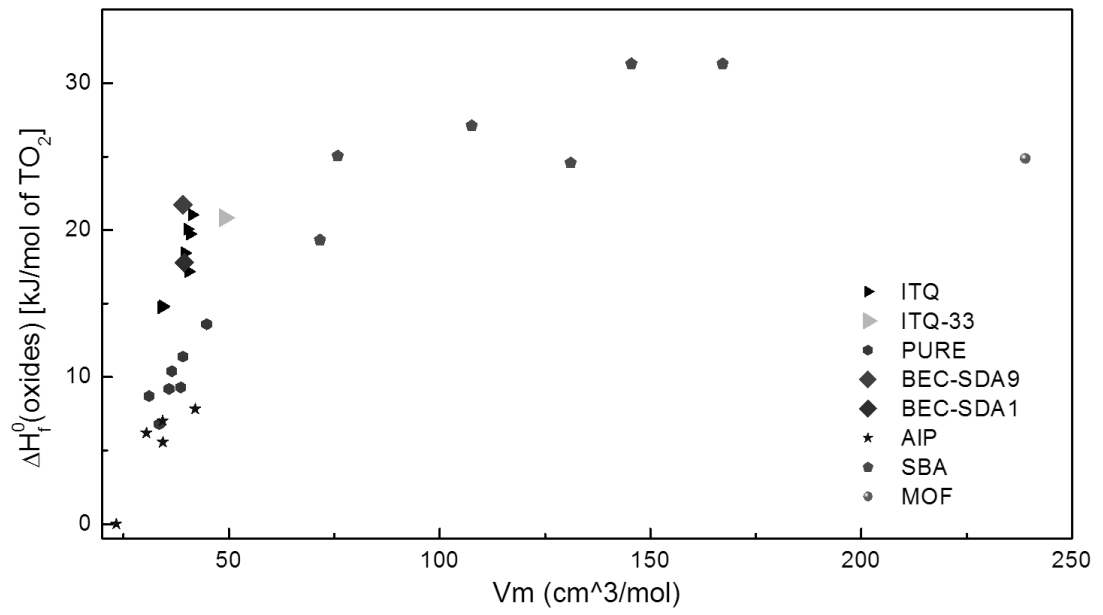


**Figure 12:** Enthalpies of formation of porous materials as a function of molar volume [11,13-15]

**Table 1.** Thermochemical cycle for ITQ-33 and pure SiO<sub>2</sub> BEC.

Reactions for ITQ-33	Enthalpy
(1) Al <sub>0.04</sub> Si <sub>0.66</sub> Ge <sub>0.3</sub> O <sub>2</sub> H <sub>0.04</sub> (s, 25°C) → 0.66SiO <sub>2</sub> (soln, 700°C) + 0.02Al <sub>2</sub> O <sub>3</sub> (soln, 25°C) + 0.02H <sub>2</sub> O (g, 700°C) + 0.3GeO <sub>2</sub> (soln, 700°C)	$\Delta H_1 = \Delta H_{ds}(\text{ITQ-33})$
(2) H <sub>2</sub> O (s, 25°C) → H <sub>2</sub> O (g, 700°C)	$\Delta H_2 = \Delta H_{hc}(\text{H}_2\text{O})$
(3) SiO <sub>2</sub> (s, 25°C) → SiO <sub>2</sub> (soln, 700°C)	$\Delta H_3 = \Delta H_{ds}(\text{SiO}_2)$
(4) Al <sub>2</sub> O <sub>3</sub> (s, 25°C) → Al <sub>2</sub> O <sub>3</sub> (soln, 700°C)	$\Delta H_4 = \Delta H_{ds}(\text{Al}_2\text{O}_3)$
(5) GeO <sub>2</sub> (s, 25°C) → GeO <sub>2</sub> (soln, 700°C)	$\Delta H_5 = \Delta H_{ds}(\text{GeO}_2)$
(6) 0.66SiO <sub>2</sub> (s, 25°C) + 0.02Al <sub>2</sub> O <sub>3</sub> (s, 25°C) + 0.02H <sub>2</sub> O (s, 25°C) + 0.3GeO <sub>2</sub> (s, 25°C) = Al <sub>0.04</sub> Si <sub>0.66</sub> Ge <sub>0.3</sub> O <sub>2</sub> H <sub>0.04</sub> (s, 25°C)	$\Delta H_6 = \Delta H_{f,ox}(\text{ITQ-33})$
$0.02\Delta H_2 + 0.66\Delta H_3 + 0.02\Delta H_4 + 0.3\Delta H_5 - \Delta H_1 = \Delta H_6 = \Delta H_{f,ox}$	
<b>Reactions for pure SiO<sub>2</sub> BEC</b>	
(7) SiO <sub>2</sub> (s, 25°C) → SiO <sub>2</sub> (soln, 700°C)	$\Delta H_7 = \Delta H_{ds}(\text{BEC})$
(8) SiO <sub>2</sub> (quartz, 25°C) → SiO <sub>2</sub> (soln, 700°C)	$\Delta H_8 = \Delta H_{ds}(\text{Quartz})$
(9) SiO <sub>2</sub> (quartz, 25°C) → SiO <sub>2</sub> (s, 700°C)	$\Delta H_9 = \Delta H_{f,ox}(\text{BEC})$
$\Delta H_8 - \Delta H_7 = \Delta H_9 = \Delta H_{f,ox}$	

**Table 2.** Enthalpies of drop solution and formation for component oxides, ITQ-33 and pure SiO<sub>2</sub> BECs

<b>Material</b>	<b>Formula</b>	<b><math>\Delta H_{ds}(\text{kJ}\cdot\text{mol}^{-1})</math></b>	<b><math>\Delta H_{f,ox}(\text{kJ}\cdot\text{mol}^{-1})</math></b>
<b>Quartz</b>	SiO <sub>2</sub>	39.10±0.30 <sup>a</sup>	0
<b><math>\alpha</math>-Alumina</b>	Al <sub>2</sub> O <sub>3</sub>	107.90±1.00 <sup>a</sup>	0
<b>Water</b>	H <sub>2</sub> O	68.90±0.10 <sup>a</sup>	0
<b>Germania (quartz structure)</b>	GeO <sub>2</sub>	25.10 ± 0.30 <sup>b</sup>	0
<b>ITQ-33</b>	Al <sub>0.04</sub> Si <sub>0.66</sub> Ge <sub>0.30</sub> O <sub>2</sub> H <sub>0.04</sub>	15.75(9) ± 0.85 <sup>c</sup>	22.12 ± 0.91
<b>Quartz</b>	SiO <sub>2</sub>	39.10 ± 0.30 <sup>a</sup>	0
<b>BEC(SDA-1)</b>	SiO <sub>2</sub>	21.31(8)±0.66 <sup>c</sup>	17.79±0.72
<b>BEC(SDA-9)</b>	SiO <sub>2</sub>	17.37(3)±2.33 <sup>c</sup>	21.73±2.35

<sup>a</sup> Ref. [15]

<sup>b</sup> Ref. [16]

c. number in ( ) is number of experiments performed, error is two standard deviations of the mean